INTERNATIONAL JOURNAL OF INTEGRATED ENGINEERING
ISSN: 2229-838X e-ISSN: 2600-7916

IJIE

Vol. 17 No. 3 (2025) 223-229
https://publisher.uthm.edu.my/ojs/index.php/ijie

Annealing Environment Dependence of Solution-Immersion Grown Nickel Oxide Nanoflowers

N. Parimon[1]*, M. H. Mamat[2,3], M. F. Malek[3,4], M. N. Afnan Uda[5]

[1] *Centre of Research in Energy and Advanced Materials, Faculty of Engineering, Universiti Malaysia Sabah, 88400 Kota Kinabalu, Sabah, MALAYSIA*
[2] *NANO-ElecTronic Centre, Faculty of Electrical Engineering, Universiti Teknologi MARA, 40450 Shah Alam, Selangor, MALAYSIA*
[3] *NANO-SciTech Lab, Centre for Functional Materials and Nanotechnology, Institute of Science, Universiti Teknologi MARA, 40450 Shah Alam, Selangor, MALAYSIA*
[4] *Faculty of Applied Sciences, Universiti Teknologi MARA, 40450 Shah Alam, Selangor, MALAYSIA*
[5] *Faculty of Engineering, Universiti Malaysia Sabah, 88400 Kota Kinabalu, Sabah, MALAYSIA*

*Corresponding Author: fara2012@ums.edu.my
DOI: https://doi.org/10.30880/ijie.2025.17.03.024

Article Info

Received: 6 August 2024
Accepted: 16 April 2025
Available online: 19 September 2025

Keywords

Nickel oxide, annealing environment, argon gas, ambient atmosphere

Abstract

Herein, nickel oxide (NiO) nanoflowers with improved crystallinity were grown on the NiO seed-coated glass substrates using different annealing environments. An atmosphere of argon (Ar) gas was used during the heat treatment process of the sample, and compared with another sample annealed in an ambient atmosphere. The effects on the structural and optical properties of NiO nanoflowers were then investigated. The properties of NiO nanoflowers annealed at 500 °C in an Ar and ambient atmosphere surrounding were analysed using X-ray diffraction (XRD), field emission scanning electron microscopy, and ultraviolet-visible spectroscopy. The XRD patterns of the highly porous NiO nanoflowers showed they were in a cubic NiO-type polycrystalline structure. The average crystallite sizes estimated from the three most prominent peaks of XRD were quite similar, with 19.0 nm and 19.4 nm for the samples annealed in the ambient and Ar environments, respectively. The dislocation density is slightly higher for the sample annealed in Ar. The optical properties demonstrated that the average transmittance in the visible region was approximately 32% and 37% for the NiO samples annealed in the ambient and Ar environments, respectively. Further, the absorbance spectra showed a higher absorption edge when the sample was annealed in the Ar atmosphere, which is 410 nm compared to 360 nm when annealed in the ambient environment.

1. Introduction

The binary semiconductor compounds, especially metal oxide semiconductors, are made up of n-type and p-type, whose film deposition can be made by various techniques. Most metal oxides commonly engaged are zinc oxide, titanium dioxide, stannic oxide, cupric oxide, and nickel oxide (NiO), which can be used in many application branches. Among the p-type metal oxide materials, NiO is one of the favourable candidates that has been extensively studied. NiO has been reported to have a wide bandgap (E_g) between 3.6 to 4.0 eV [1], [2] and has a

particular specialty that can be used in different potential device applications such as sensors [3], [4] as well as electrochromic devices [5] and organic light-emitting diodes (OLED) [6].

During the deposition or growth process of the film, deficiencies in terms of oxidation and impurities might occur [7]. According to Yang et al. [1], the influence of the oxidation state of the cation under different ambient conditions may vary the physical properties of the transition metal oxides. Besides, the presence of impurities typically leads to a decrease in the melting point of certain bulk substances. One of the ways to change the properties of the metal oxide semiconductors is to diversify the annealing process applied in different environments, in which the process normally takes place after the growth or deposition process. In other words, the post-annealing treatment is the standard parameter that can influence the nature of the material and further enhance its crystallinity [8], [9]. For instance, by providing argon (Ar) as an isolated ambient gas, the contaminants could be removed, and crystal defects coming from the external ambient can be eliminated. As such, the conductivity and transparency of the film could be improved, and the resistive properties could also be lowered, thus making a certain device application more stable and efficient [7].

Many existing studies have been intensively reported on the different annealing temperatures and various fabrication techniques of NiO [10]. Nonetheless, not many have researched the annealing temperature in different environments to see the effect on the physical properties of NiO. Hence, this work presents the properties of NiO nanoflowers that grew using the solution-immersion method and were annealed at 500 °C under ambient and Ar environments. Then, the influence of annealing in these environments on the structural and optical properties of the samples was observed and investigated.

2. Methodology

2.1 Synthesis of NiO Nanoflowers

The sample preparation used two-step processes: the sol-gel spin coating and solution-immersion growth processes. These processes are quite similar to the previous studies by Parimon et al. [4], [11], where immersion is their predominant method. Before NiO nanoflowers grew, the NiO seed layer (SL) was deposited on the glass substrate using the sol-gel spin coating technique. The SL solution containing chemicals of nickel acetate (precursor), diethanolamine (stabiliser), and ethylene glycol monoethyl ether (solvent) was stirred for 2 hours before the spin coating process was conducted. Then, the SL was dried at 150 °C for 5 minutes. The processes of spin-coating and heating were repeated five times before the two seed-coated samples were annealed at 400 °C for 2 hours. The next step was the growth of NiO nanoflowers by the immersion method at 95 °C for 2 hours, where the nickel nitrate hexahydrate, hexamethylenetetramine, and deionised water were used as the solution. The solution underwent the sonication and stirring processes before the samples were immersed. Further, the available NiO nanoflowers were pre-baked at 150 °C in a furnace and annealed at 500 °C for 1 hour in the ambient and Ar environments, respectively. The annealing in the ambient atmosphere was done inside the furnace (Protherm), as shown in Fig. 1(a), while the annealing in the Ar environment was done in the chemical vapour deposition (CVD), STF 40-1100, as shown in Fig. 1(b). To ensure the absence of oxygen in CVD, the Ar flowed into the furnace at a gas flow rate of 100, with the samples placed inside before starting the annealing procedure. Both types of equipment used during the annealing process for NiO nanoflower samples are shown in Fig. 1.

(a) **(b)**

Fig. 1 *Annealing treatment at 500 °C of NiO nanoflowers in: (a) furnace for ambient atmosphere; and (b) CVD for 100 flow rate, Ar gas environment*

Int. Journal of Integrated Engineering Vol. 17 No. 3 (2025) p. 223-229

2.2 Characterisation of NiO Nanoflowers

The measurement only involved structural and optical characterisation. The surface morphological studies of the samples were conducted using a field emission scanning electron microscope (FESEM), Zeiss Supra 40VP. The polycrystalline structures of NiO nanoflowers were analysed using X-ray diffraction (XRD) patterns, PANalytical X'Pert PRO. Meanwhile, the ultraviolet-visible (UV-vis) spectrophotometer, Jasco/V-670 EX, is used to examine their optical properties.

3. Results and Discussion

3.1 Structural Properties

The XRD measurement was conducted to investigate the crystalline quality of the NiO nanoflowers that were deposited on the NiO SL and annealed under different environments. As shown in Fig. 2, the XRD patterns indicate that both NiO nanoflower samples display polycrystalline structures, which can be indexed to the cubic type of β-NiO (JCPDS NO.47-1049). Both samples show three prominent diffraction peaks at 2θ values of approximately 36.7°, 42.7°, and 62.4°, which were indexed to (111), (200), and (220) crystal planes, respectively. Meanwhile, two infirm diffraction peaks at 75.0° and 79.1° were indexed to (311) and (222), respectively. Among the two diffraction patterns exhibited, the three highest diffraction intensities at (111), (200), and (220) crystal planes were detected in the sample annealed in an Ar environment. It shows that the sample had a higher crystallisation and led to the successful growth of NiO at 500 ºC-annealed under the Ar environment compared to the ambient atmosphere. In other words, the crystallinity improved with Ar-annealing compared to ambient atmosphere-annealing.

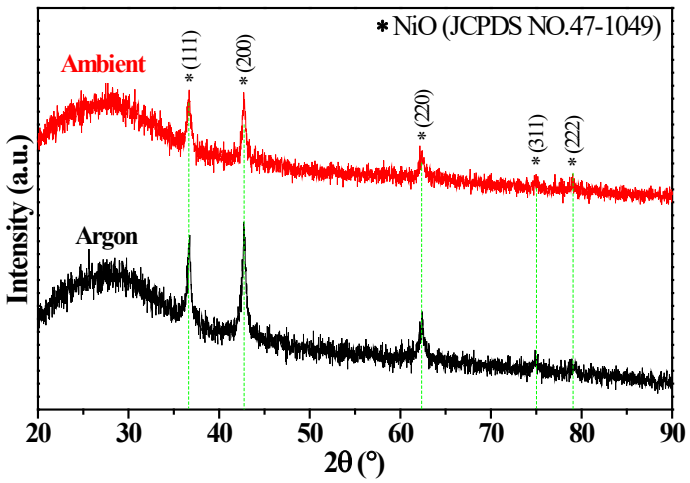

Fig. 2 *The XRD patterns of NiO nanoflowers annealed at 500 °C in the ambient atmosphere and Ar gas*

As supported by Park et al. [12], using Ar as the ambient gas during the heat treatment improves the diffraction peak intensity. In other research stated by Wang et al. [13], the enhanced crystallinity and high defect state can cause good photovoltaic properties in terms of the efficiency of solar cells. It shows that certain performance for any applications can be optimised when the crystallinity improves. The crystallite size (D) could be assessed using the Scherrer Eq. (1) from the measured FWHM (β) values (in radians). λ is the X-ray wavelength with 1.54 Å, and θ is the diffraction angle.

$$D = \frac{0.94\lambda}{\beta\cos(\theta)} \tag{1}$$

The D values from the three crystal planes of the samples were calculated and recorded in Table 1. The results show that the average D values for both samples are quite similar, with the Ar-annealed sample being slightly higher. This result was followed by the average dislocation density (δ), which shows a similar trend and is summarised in Table 2. This δ can be calculated through Eq. (2), which measures the number of dislocations per unit area in a crystal. The higher δ, the higher distortions in the atomic arrangement, which implies a high degree of defectiveness. A higher degree of defectiveness can sometimes enhance the electrical and thermal conductivity of the materials. From the higher number of defects, the force of attraction between delocalized electrons and nuclei will increase the stability of the NiO nanoflower that is annealed in Ar [14].

$$\delta = \frac{1}{D^2} \tag{2}$$

Table 1 *The average crystallite size at (111), (200), and (220) crystal planes*

Sample Annealed	Crystallite Size, D (nm)			Average D (nm)
	(1 1 1)	(2 0 0)	(2 2 0)	
Ambient	17.7	21.4	18.0	19.0
Argon	23.4	17.5	17.2	19.4

Table 2 *The average dislocation density at (111), (200), and (220) crystal planes*

Sample Annealed	Dislocation density, $\delta \times 10^{15}$ (Lines/m^2)			Average δ $\times 10^{15}$ (Lines/m^2)
	(1 1 1)	(2 0 0)	(2 2 0)	
Ambient	3.182	2.183	3.088	2.818
Argon	1.829	3.263	3.381	2.824

3.2 Morphological Properties

As shown in Fig. 3, the surface morphological images of NiO nanoflowers at different annealing environments revealed that their shape and pattern were similar to flower-like nanostructures with very thin and porous petals. The unique structure with a bouquet of rounded flowers can be observed to be the same as the nanocarnation-like and nanoflower NiO reported by Parimon et al. [15], [16]. In addition, the average diameter of an individual flower-like NiO is also the same for both annealing environments, of approximately 1.5 µm. As shown in Fig. 3(a) and Fig. 3(b), the NiO nanoflower images refer to the magnification of 10 k × and 50 k × for ambient atmosphere-annealed samples, respectively. Whereas in Fig. 3(c) and Fig. 3(d), the NiO nanoflower images refer to the magnification of 10 k × and 50 k × for Ar gas-annealed samples, respectively. These images revealed that more prominent petals and porous matter could be seen in the sample annealed in the Ar environment than in the sample annealed in the ambient environment. Meanwhile, Fig. 4 shows the energy-dispersive X-ray analysis (EDX) for the sample annealed in Ar. Well-defined peaks for nickel (Ni) and oxygen (O) can be observed. In addition, there are two lower peaks, silicon (Si) from the glass substrate and Ar from the annealing environment.

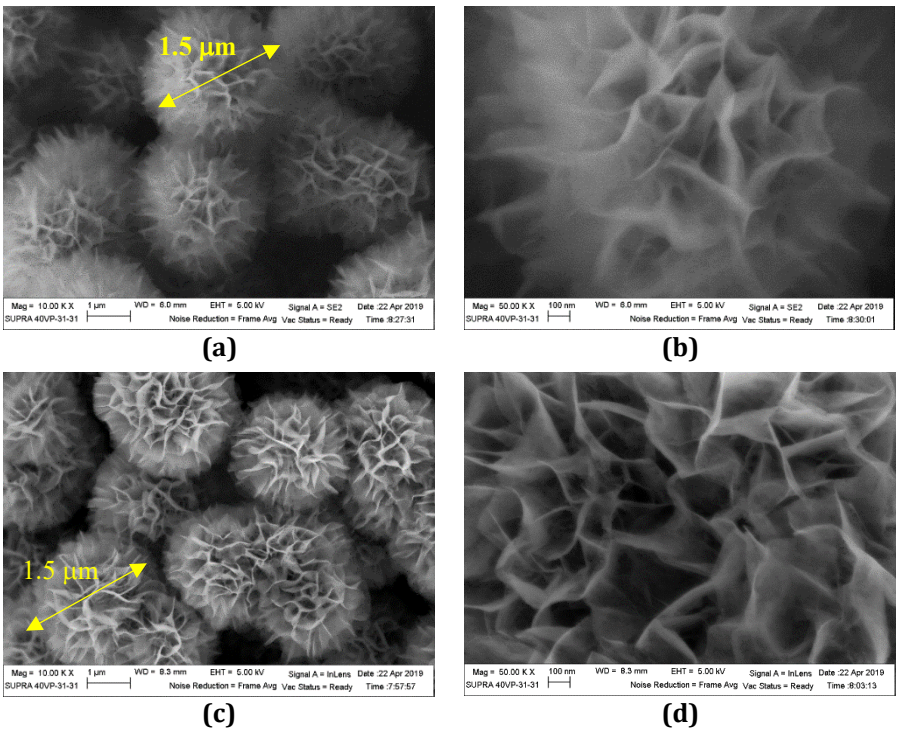

Fig. 3 *The FESEM images of NiO nanoflowers annealed at 500 °C in: (a) and (b) ambient atmosphere; and (c) and (d) Ar gases*

Int. Journal of Integrated Engineering Vol. 17 No. 3 (2025) p. 223-229

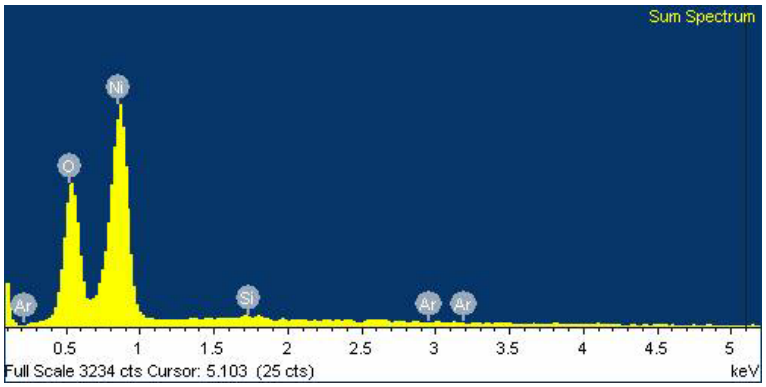

Fig. 4 *Energy dispersive X-ray analysis for Ar-annealed sample*

3.2.1 Optical Properties

Fig. 5(a) and Fig. 5(b) demonstrate the optical transmittance and absorbance of the NiO nanoflowers at different annealing environments, respectively. The transmittance plot shows that the NiO nanoflowers exhibit transparency in the visible region with a slightly higher value when annealed in the Ar ambient than when annealed in the ambient atmosphere. The average transmittance percentage value in the visible region (VR) ~ (400 – 800 nm) was estimated to be at 32% and 37% for the ambient and Ar environments, respectively. It can be seen that both optical transmissions are less than 50 %. The lowest transmittance percentage in the ambient environment may be due to the greater nanoflower thickness than that of annealing in an Ar environment [4]. It shows that the changes in optical properties could be related to the variation in thickness after annealing in different atmospheres.

The absorbance spectra in Fig. 5(b) revealed that NiO nanoflowers exhibit different optical absorption values. The absorption in the VR can be related to some local energy levels caused by intrinsic defects [17]. According to Cergel et al. [18], the increase in absorption value depends on the oxygen vacancies on the nanostructure surfaces due to the annealing environment. In addition, the spectra show the UV absorption edges at a wavelength below 410 nm for the Ar-annealed sample, while the absorption edge is below 360 nm for the ambient atmosphere-annealed sample. The optical absorption at the absorption edge correlated with the transition from the valence band to the conduction band [17]. From the results, it can be postulated that the optical properties can be changed by using different gases in the annealing process. For instance, the optical bandgap of the sample annealed in the Ar environment can be considerably smaller than that of the sample annealed in the ambient atmosphere.

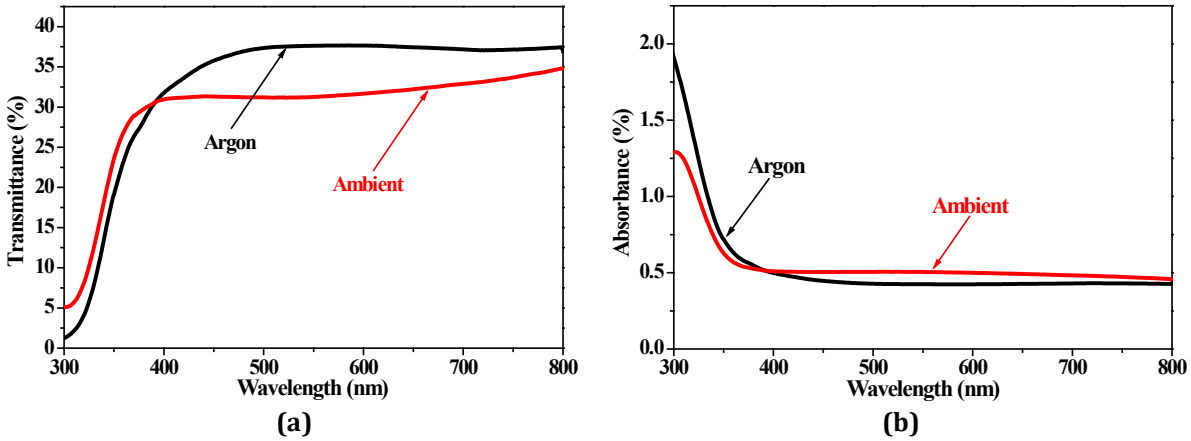

Fig. 5 *NiO nanoflowers at 500 °C in different annealing environments: (a) transmittance; and (b) absorbance*

4. Conclusion

The effects of annealing environments on the structural and optical properties of NiO nanoflowers prepared via a solution-grown immersion method were studied. The annealing environment treatment was performed at 500 °C for 1 hour under the ambient atmosphere and isolated Ar gas. The surface morphologies show that the nanoflower shape of NiO annealed in Ar is more prominent and porous than in the ambient atmosphere. From the XRD patterns and optical properties, NiO annealed in the Ar environment exhibits improved crystallinity and high transparency compared to the sample annealed in an ambient atmosphere. A higher crystallite size was produced

in the Ar atmosphere, generating a higher density of defects. The absorption edge in the sample annealed in the Ar environment is at a longer wavelength than in the ambient environment. In conclusion, both NiO samples annealed in different environments have comparable structural and morphological characteristics. They may be applied in possible applications, such as photovoltaic devices, sensors, and electrochemical devices. Therefore, further optimisation and characterisation of NiO are needed to achieve the best results for each application.

Acknowledgement

This research was funded by the Skim Penyelidikan Bidang Keutamaan (SBK0511-2022), an internal grant of UMS. The authors thank the NANO-ElecTronic Centre (NET) at the Faculty of Electrical Engineering, UiTM Shah Alam, for providing the laboratory facilities to run this experiment.

Conflict of Interest

The authors declare that there is no conflict of interest regarding the publication of the paper.

Author Contribution

The authors confirm contribution to the paper as follows: ***study conception and design:*** *N. Parimon, M. H. Mamat;* ***data collection:*** *M. F. Malek;* ***analysis and interpretation of results:*** *N. Parimon, M. N. Afnan Uda;* ***draft manuscript preparation:*** *N. Parimon, M. H. Mamat. All authors reviewed the results and approved the final version of the manuscript.*

References

[1] Yang, S., Kim, J., Choi, Y., Kim, H., Lee, D., Bae, J. S., & Park, S. (2020). Annealing environment dependent electrical and chemical state correlation of Li-doped NiO. Journal of Alloys and Compounds, 815, 152343. https://doi.org/10.1016/j.jallcom.2019.152343

[2] Mamat, M. H., Parimon, N., Ismail, A. S., Shameem Banu, I. B., Sathik Basha, S., Vijayaraghavan, G. V., Yaakob, M. K., Suriani, A. B., Ahmad, M. K., & Rusop, M. (2019). Structural, optical, and electrical evolution of sol–gel-immersion grown nickel oxide nanosheet array films on aluminium doping. Journal of Materials Science: Materials in Electronics, 30, 9916-9930. https://doi.org/10.1007/s10854-019-01330-z

[3] Yin, M., & Zhu, Z. (2019). Mesoporous NiO as an ultra-highly sensitive and selective gas sensor for sensing of trace ammonia at room temperature. Journal of Alloys And Compounds, 789, 941-947. https://doi.org/10.1016/j.jallcom.2019.03.143

[4] Parimon, N., Mamat, M. H., Ismail, A. S., Banu, I. S., Ahmad, M. K., Suriani, A. B., & Rusop, M. (2020). Influence of annealing temperature on the sensitivity of nickel oxide nanosheet films in humidity sensing applications. Indonesian Journal of Electrical Engineering and Computer Science, 18, 284-292. http://doi.org/10.11591/ijeecs.v18.i1.pp284-292

[5] Zrikem, K., Song, G., Aghzzaf, A. A., Amjoud, M., Mezzane, D., & Rougier, A. (2019). UV treatment for enhanced electrochromic properties of spin coated NiO thin films. Superlattices and Microstructures, 127, 35-42. https://doi.org/10.1016/j.spmi.2018.03.042

[6] Tsai, C. T., Wang, C. T., Chen, Y. Y., Kao, P. C., & Chu, S. Y. (2019). Improved hole-injection and external quantum efficiency of organic light-emitting diodes using an ultra-thin K-doped NiO buffer layer. Journal of Alloys and Compounds, 797, 159-165. https://doi.org/10.1016/j.jallcom.2019.05.058

[7] Urper, O., Karacasu, O., Cimenoglu, H., & Baydogan, N. (2019). Annealing ambient effect on electrical properties of ZnO: Al/p-Si heterojunctions. Superlattices and Microstructures, 125, 81-87. https://doi.org/10.1016/j.spmi.2018.10.027

[8] Souici, F. Z., Benhaoua, B., SAÏDId, H., Boujmil, M. F., Rahal, A., Benhaoua, A., & Aida, M. S. (2019). Influence of rapid thermal annealing in argon atmosphere on properties of electrodeposited $CuInSe_2$ thin films: Structural and optical stady. Chalcogenide Letters, 16, 79-87.

[9] Sobri, M., Shuhaimi, A., Hakim, K. M., Ganesh, V., Mamat, M. H., Mazwan, M., Najwa, S., Ameera, N., Yusnizam, Y., & Rusop, M. (2014). Effect of annealing on structural, optical, and electrical properties of nickel (Ni)/indium tin oxide (ITO) nanostructures prepared by RF magnetron sputtering. Superlattices and Microstructures, 70, 82-90. https://doi.org/10.1016/j.spmi.2014.02.010

[10] Parimon, N., Mamat, M. H., Banu, I. S., Vasimalai, N., Ahmad, M. K., Suriani, A. B., Mohamed, A., & Rusop, M. (2021). Annealing temperature dependency of structural, optical and electrical characteristics of manganese-doped nickel oxide nanosheet array films for humidity sensing applications. Nanomaterials and Nanotechnology. https://doi.org/10.1177/1847980420982788

[11] Parimon, N., Mamat, M. H., & Rusop, M. (2022). Undoped and Zn-doped NiO nanosheet/nanoflower-like films-based humidity sensor fabricated via immersion method. Materials Today: Proceedings, 48, 1910-1914. https://doi.org/10.1016/j.matpr.2021.09.364

[12] Park, D. J., Lee, J. Y., Park, T. E., Kim, Y. Y., & Cho, H. K. (2007). Improved microstructural properties of a ZnO thin film using a buffer layer in-situ annealed in argon ambient. Thin Solid Films, 515, 6721-6725. https://doi.org/10.1016/j.tsf.2007.01.047

[13] Wang, B., Wong, K. Y., Yang, S., & Chen, T. (2016). Crystallinity and defect state engineering in organo-lead halide perovskite for high-efficiency solar cells. Journal of Materials Chemistry A, 4, 3806-3812. https://doi.org/10.1039/C5TA09249C

[14] Gomathi, M., Rajkumar, P. V., & Prakasam, A. (2018). Study of dislocation density (defects such as Ag vacancies and interstitials) of silver nanoparticles, green-synthesized using Barleria cristata leaf extract and the impact of defects on the antibacterial activity. Results in Physics, 10, 858-864. https://doi.org/10.1016/ j.rinp.2018.08.011

[15] Parimon, N., Mamat, M. H., Abdullah, M. A. R., Ismail, A. S., Ahmad, W. R. W., Banu, I. S., & Rusop, M. (2018). Nanocarnation-like nickel oxide thin film: structural and optical properties. International Journal of Engineering & Technology, 7, 103-106. https://doi.org/10.14419/IJET.V7I4.18.21831

[16] Parimon, N., Mamat, M. H., Ahmad, M. K., Banu, I. S., & Rusop, M. (2019). Highly porous NiO nanoflower-based humidity sensor grown on seedless glass substrate via one-step simplistic immersion method. International Journal of Engineering and Advanced Technology, 9, 5718-5722. https://doi.org/10.35940/ijeat.A3052. 109119

[17] Benramache, S., Aoun, Y., Gacema, R., & Mourghadea, H. (2021). Synthesis and annealing temperature effect on structural, optical and electrical properties of NiO thin films deposited by sol–gel technique. Nanosistemi, Nanomateriali, Nanotehnologii, 19, 147-158.

[18] Söyleyici Cergel, M., & Atay, F. (2019). The role of the annealing process in different gas environments on the degradation of the methylene blue organic pollutant by brookite-TiO2 photocatalyst. Ionics, 25, 3823-3836. https://doi.org/10.1007/s11581-019-02941-6